Attenuation compensation technique and rainfall rate estimation using *C*-band dual polarization radar

G. SCARCHILLI ([1]), E. GORGUCCI ([1]), G. GALATI ([2]) and G. PAVAN ([2])

([1]) *Istituto di Fisica dell'Atmosfera (CNR) - Via del Fosso del Cavaliere, 00133, Roma, Italy*
([2]) *Univerisità di "Tor Vergata" and Centro "Vito Volterra" Via di Tor Vergata snc, 00133, Roma, Italy*

(ricevuto il 10 Giugno 1996, approvato il 3 Marzo 1998)

Summary. — The effectiveness of an attenuation correction procedure on the error structure of a *C*-band radar rainfall estimation is studied theoretically and by computer simulation. The iterative procedure to correct the radar observables affected by attenuation is based on the best-fit relationships between the absolute and differential reflectivity and the specific absolute and differential attenuation. This paper evaluates this attenuation correction procedure by a computer simulation to value the rainfall rate estimation errors.

PACS 92.40.Ea – Precipitation.
PACS 92.60 – Meteorology.

List of symbol and notations

$r^{(v)}$	*True* rainrate.
$r^{(p)}$	Parametrized rain, estimate of rainrate by best-fit relationship using *true* values of Z_H and Z_{DR}.
$r^{(c)}$	Estimate of *attenuation-corrected* rainrate (by *corrected* values of Z_H and Z_{DR}).
$[r^{(p)}]_n$	Parametrized rain, estimate of rainrate by best-fit relationship at the n-th cell using Z_H and Z_{DR}.
$[r^{(c)}]_n$	Estimate of *attenuation-corrected* rainrate at the n-th cell (by *corrected* values of Z_H and Z_{DR}).
$[Z_H^{(v)}]_n$	*True* reflectivity factor at H polarization at the n-th cell.
$[Z_{DR}^{(v)}]_n$	*True* differential reflectivity at the n-th cell.
$[Z_H^{(m)}]_n$	*Measured* (attenuated) reflectivity factor at H polarization at n-th cell.
$[Z_{DR}^{(m)}]_n$	*Measured* (attenuated) differential reflectivity at the n-th cell.
$[Z_H^{(c)}]_n$	*Attenuation-corrected* reflectivity factor at H polarization at n-th cell.
$[Z_{DR}^{(c)}]_n$	*Attenuation-corrected* differential reflectivity at the n-th cell.
$\widehat{\alpha}_{H_i}$	Estimate of specific attenuation at H polarization by best-fit relationship at the i-th cell.
$\widehat{\alpha}_{D_i}$	Estimate of specific differential attenuation by best-fit relationship at the i-th cell.
Δx_i	The i-th cell length.

L	Propagation path (one way).
ε	Error per cent.
$[\varepsilon]_n$	Error per cent of the n-th.
FSE	Fractional Standard Error.
$N(D)$	Drop Size Distribution.
DSD	Acronym of the Drop Size Distribution.
N_0	Gamma DSD scale parameter.
D_0	Gamma DSD parameter (median diameter).
μ	Gamma DSD shape parameter.

1. – Introduction

In the last years there has been an increasing interest in polarimetric radar measurements for meteorological remote-sensing applications.

As is known, it is possible to estimate the rainfall rate utilizing the reflectivity factor and differential reflectivity, or the differential phase shift along the rain-filled path.

However, at C-band wavelengths reflectivity measurements are affected by attenuation of radar signals passing through the precipitation that exists between the radar and the measurement cell. Differential-reflectivity measurements at C-band are similarly affected by the differential attenuation between H and V polarised waves. Experimental measurements have shown that the absolute specific attenuation α_{H} and the differential specific attenuation α_{D} through extended rain cells could be of 0.5 dB/km and 0.1 dB/km, respectively when the rainrate is around 100 mm/h [1].

This problem was studied by Hildebrand [2]. He proposed at C-band an iterative attenuation correction scheme in which the attenuation at each rain cell was estimated from the attenuation-corrected reflectivity factor at that cell. He concluded that for a radar calibrated to within 2 dB this procedure should be used only in storms with $45 \leqslant Z_{\mathrm{H}} \leqslant 60$ dBZ.

For dual polarization C-band radars Aydin *et al.* [3, 4] suggested an attenuation estimation procedure where α_{H} and α_{D} were estimated using disdrometer-based simulations. They concluded that the procedure is very sensitive to biases, which include calibration errors, in the measurements of Z_{H} and Z_{DR}.

Gorgucci *et al.* [5] proposed a direct simple approach to estimate α_{H} and α_{D} based on Z_{H} and Z_{DR} measurements. Their technique is based on a cumulative scheme, in which the attenuation at the n-th cell is estimated using the attenuation-corrected reflectivity Z_{H} and Z_{DR} at the previous cell.

This paper evaluates this attenuation correction procedure by a computer simulation to value the rainfall rate estimation errors; moreover, we compare the accuracy of (Z_{H}, Z_{DR}) rainfall-based estimates with those based on K_{DP} measurements, assuming that the influence of back-scatter differential phase is negligible.

2. – Meteorological radar observables

Here are the definitions of the meteorological radar observables:

Rainfall rate

$$r = 0.6 \cdot 10^{-3} \pi \int D^3 v(D)\, N(D)\, \mathrm{d}D \quad (\mathrm{mm/h}). \tag{1}$$

Reflectivity factor at horizontal (H) and vertical (V) polarization:

$$Z_{\mathrm{H,V}} = 10\ \log_{10}\left[\frac{\lambda^4}{\pi^5 |K|^2}\int \sigma_{\mathrm{H,V}}(D)\, N(D)\, \mathrm{d}D\right] \quad (\mathrm{dB}\,Z). \tag{2}$$

Differential reflectivity between horizontal (H) and vertical (V) polarization:

$$Z_{\mathrm{DR}} = Z_{\mathrm{H}} - Z_{\mathrm{V}} \quad (\mathrm{dB}). \tag{3}$$

Specific differential phase shift between horizontal (H) and vertical (V) polarization:

$$K_{\mathrm{DP}} = \frac{180}{\pi}\lambda\, \mathrm{Re}\left\{\int [f_{\mathrm{H}}(D) - F_{\mathrm{V}}(D)]\, N(D)\, \mathrm{d}D\right\} \quad (\mathrm{deg/km}). \tag{4}$$

Specific attenuation at horizontal (H) and vertical (V) polarization:

$$\alpha_{\mathrm{H,V}} = 8.686\,\lambda\, \mathrm{Im}\left\{\int f_{\mathrm{H,V}}(D)\, N(D)\, \mathrm{d}D\right\} \quad (\mathrm{dB/km}). \tag{5}$$

Specific differential attenuation between horizontal (H) and vertical (V) polarization:

$$\alpha_D = \alpha_{\mathrm{H}} - \alpha_{\mathrm{V}} \quad (\mathrm{dB/km}), \tag{6}$$

where D is the equivolumetric spherical diameter of a raindrop.

In eqs. (1), (2), (4) and (5) $N(D)$ is the number of raindrops per unit volume per unit size interval (D to $D + \Delta D$) and can be adequately described by a *Gamma* model given by

$$N(D) = N_0 D^{\mu} \exp\left[-\frac{3.67 + \mu}{D_0} D\right], \tag{7}$$

where the parameters N_0, D_0 and μ of DSD can vary over a wide range as suggested by Ulbrich [6]:

$$10^{3.2-\mu} \exp[2.8\,\mu] \leqslant N_0 \leqslant 10^{4.5-\mu} \exp[3.57\,\mu] \quad (\mathrm{m^{-3}\,mm^{-1-\mu}}), \tag{8a}$$

$$0.5 \leqslant D_0 \leqslant 2.5 \quad (\mathrm{mm}), \tag{8b}$$

$$-1 < \mu \leqslant 4. \tag{8c}$$

In eq. (1) $v(D)$ is the fall speed of raindrop related to D(mm) by the following relationship: $v(D) = 3.778\, D^{0.67}$ (m/s). In eq. (2) $\sigma_{\mathrm{H,V}}(D)$ represent the radar cross-sections at horizontal and vertical polarization, respectively, λ is the wavelength and $K = (\varepsilon_r - 1)/(\varepsilon_r + 2)$, where ε_r is the complex refractive index of water (for a fixed temperature). In eqs. (4) and (5) $f_{\mathrm{H,V}}(D)$ are the forward-scatter amplitudes at H and V polarization, respectively.

Assuming a *Gamma* distribution eq. (7), after integration of eq. (1), the *true* rainfall rate can be written as

$$r^{(v)} = 0.6\,\pi \cdot 10^{-3} N_0 \cdot 3.778 \cdot \frac{\Gamma(\mu + 4.67)}{\Lambda^{\mu + 4.67}}, \tag{9}$$

where the parameter Λ is related to D_0 by the relation: $\Lambda = (3.67 + \mu)/D_0$ and $\Gamma(\cdot)$ is

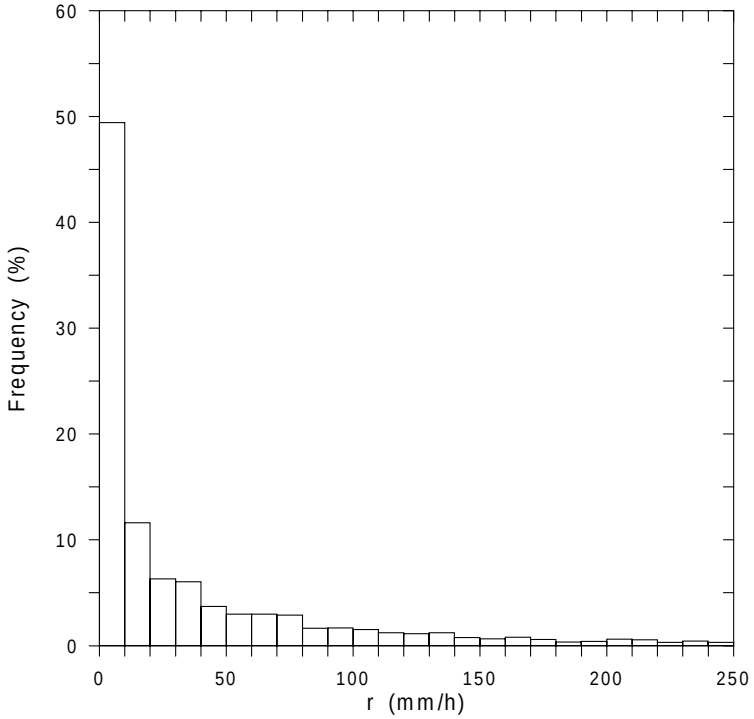

Fig. 1. – Rainrate histogram (4000 trials), Gamma DSD parameters are varied over the Ulbrich range.

the *Gamma*-function. Utilizing the limits described in (8*a*), (8*b*) and (8*c*), in fig. 1 the simulated rainrate histogram is shown. The number of trials is 4000. We can see that the rainrate is included between 0 and 20 mm/h for 60% of the trials.

The $(Z_{\mathrm{H}}, Z_{\mathrm{DR}})$ rainfall estimate can be derived by applying the following relationship (at *C*-band), proposed by Gorgucci *et al.* [5]:

$$r = c_1 \cdot 10^{c_2 Z_{\mathrm{H}}} \cdot 10^{-c_3 Z_{\mathrm{DR}}} \quad (\mathrm{mm/h}), \tag{10}$$

where $c_1 = 7.6 \cdot 10^{-3}$, $c_2 = 0.093$, $c_3 = 0.281$, with Z_{H} and Z_{DR} expressed in (dB*Z*) and (dB).

The rainfall rate can be also estimated using the best-fit relationship at *C*-band proposed by Scarchilli *et al.* [7]:

$$r = 19.8\, K_{\mathrm{DP}} \quad (\mathrm{mm/h}), \tag{11}$$

where the differential phase shift between the horizontal and vertical polarization K_{DP} (deg/km) is a non-attenuated radar observable. Then, in the following, this estimator will be considered as reference. Moreover, we remember that K_{DP} is composed of two terms related to the forward- and back-scattering; in this work the back-scattering contribution is neglected.

The performances of the estimators are evaluated by two figures: the percentage error $\varepsilon = (\sum_i (v_i - s_i)) / \sum_i v_i$ and the Fractional Standard Error, FSE =

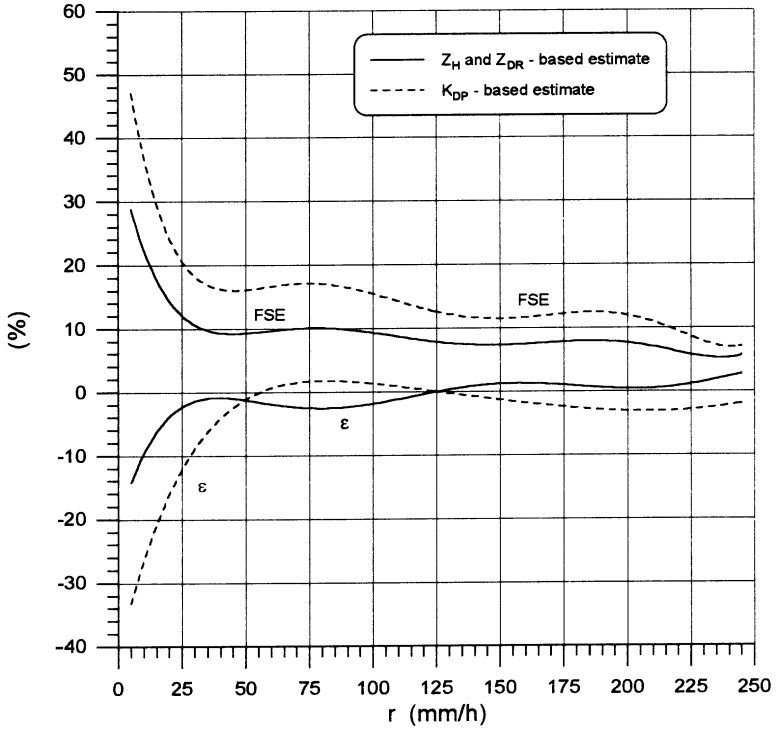

Fig. 2. – Bias ε and FSE of the rainrate estimator: solid line, eq. (10); dotted line, eq. (11); *C*-band, $T = 10\,°\mathrm{C}$.

$(\sqrt{(1/N)\sum_i (\nu_i - s_i)^2})/((1/N)\sum_i \nu_i)$, where ν_i and s_i represent the *true* and *estimated* value, respectively, and N is the sample size.

Figure 2 shows the percentage error ε and the FSE of the rainrate estimators (10) and (11) as a function of rainrate. The correlation coefficients are 0.993 and 0.982, respectively. We can see from fig. 2 that the FSE of the estimator (11) is greater than the FSE of the estimator (10) and decreases continuously with increasing rainfall rate over the entire range of r.

3. – Attenuation compensation technique

Attenuation and differential attenuation cumulatively increase with the range. Then the measured reflectivity factor $Z_{\mathrm{H}}(\mathrm{dB}\,Z)$ and the differential reflectivity $Z_{\mathrm{DR}}(\mathrm{dB})$ at the n-th range cell are related to *true* values as

$$[Z_{\mathrm{H}}^{(\mathrm{m})}]_n = [Z_{\mathrm{H}}^{(\nu)}]_n - 2\sum_{i=1}^{n-1} \alpha_{\mathrm{H}_i}\,\Delta x_i \qquad (\mathrm{dB}\,Z), \tag{12a}$$

$$[Z_{\mathrm{DR}}^{(\mathrm{m})}]_n = [Z_{\mathrm{DR}}^{(\nu)}]_n - 2\sum_{i=1}^{n-1} \alpha_{\mathrm{D}_i}\,\Delta x_i \qquad (\mathrm{dB}), \tag{12b}$$

where Δx_i is the length of the i-th range cell, the factor 2 takes account of the two-way

path, while α_{H_i} and α_{D_i} are the specific attenuation (one way) at the i-th cell. In the attenuation compensation iterative scheme the absolute attenuation and differential attenuation at i-th range cell are estimated using *attenuation-corrected values* of the reflectivity factor and differential reflectivity at previous cells. The attenuation-corrected values of horizontal reflectivity and differential reflectivity can be estimated as

$$[Z_H^{(c)}]_n = [Z_H^{(m)}]_n + 2 \sum_{i=1}^{n-1} \widehat{\alpha}_{H_i} \Delta x_i \quad (\mathrm{dB}\, Z), \tag{13a}$$

$$[Z_{DR}^{(c)}]_n = [Z_{DR}^{(m)}]_n + 2 \sum_{i=1}^{n-1} \widehat{\alpha}_{D_i} \Delta x_i \quad (\mathrm{dB}), \tag{13b}$$

where $\widehat{\alpha}_{H_i}$ and $\widehat{\alpha}_{D_i}$ are the estimates of the specific attenuation and differential attenuation. Using this scheme we suppose that the first cell is not attenuated along the propagation path.

Gorgucci *et al.* [5] proposed, at C-band, the following relationship:

$$\widehat{\alpha}_H = a_1 \cdot 10^{a_2 \cdot Z_H} \cdot 10^{a_3 \cdot Z_{DR}} \quad (\mathrm{dB/km}), \tag{14a}$$

$$\widehat{\alpha}_D = b_1 \cdot 10^{b_2 \cdot Z_H} \cdot 10^{b_3 \cdot Z_{DR}} \quad (\mathrm{dB/km}), \tag{14b}$$

where the reflectivity Z_H and Z_{DR} are in (dB Z) and (dB), respectively, while $\widehat{\alpha}_H$ and $\widehat{\alpha}_D$ are expressed in (dB/km). As is shown in table I and table II, the coefficients of eqs. (14*a*) and (14*b*) change with the temperature but their variation is not accentuated. In the following we will consider the coefficients at $T = 10$ °C.

At C-band ($f = 5.45$ GHz), figs. 3*a* and 3*b* are computed using eqs. (14*a*) and (14*b*), respectively and show the percentage error ε and the FSE of the α_H and α_D estimates when the rainrate is varied between 0 and 250 mm/h. It can be shown that the estimators $\widehat{\alpha}_H$ and $\widehat{\alpha}_D$ follow very closely the actual values. In fact, the correlation coefficients are 0.997 and 0.994, respectively. Both ε and the FSE in $\widehat{\alpha}_H$ are high for low attenuation values, then they decrease quickly and take on values, lower to 10% with

TABLE I. – *Coefficients used in eq.* (14*a*) *to estimate* $\widehat{\alpha}_H$ *for* $T = 0.5$, 2.0, 5.0, 10 *and* 20.0 °C.

T (°C)	a_1	a_2	a_3
0.5	$9.89 \cdot 10^{-6}$	0.095	− 0.130
2.0	$9.03 \cdot 10^{-6}$	0.096	− 0.124
5.0	$7.78 \cdot 10^{-6}$	0.097	− 0.119
10.0	$6.31 \cdot 10^{-6}$	0.097	− 0.104
20.0	$4.02 \cdot 10^{-6}$	0.098	− 0.080

TABLE II. – *Coefficients used in eq.* (14*b*) *to estimate* $\widehat{\alpha}_D$ *for* $T = 0.5$, 2.0, 5.0, 10 *and* 20.0 °C.

T (°C)	b_1	b_2	b_3
0.5	$6.47 \cdot 10^{-7}$	0.102	− 0.052
2.0	$6.84 \cdot 10^{-7}$	0.102	− 0.050
5.0	$6.62 \cdot 10^{-7}$	0.101	− 0.044
10.0	$5.86 \cdot 10^{-7}$	0.102	− 0.030
20.0	$5.03 \cdot 10^{-7}$	0.101	− 0.011

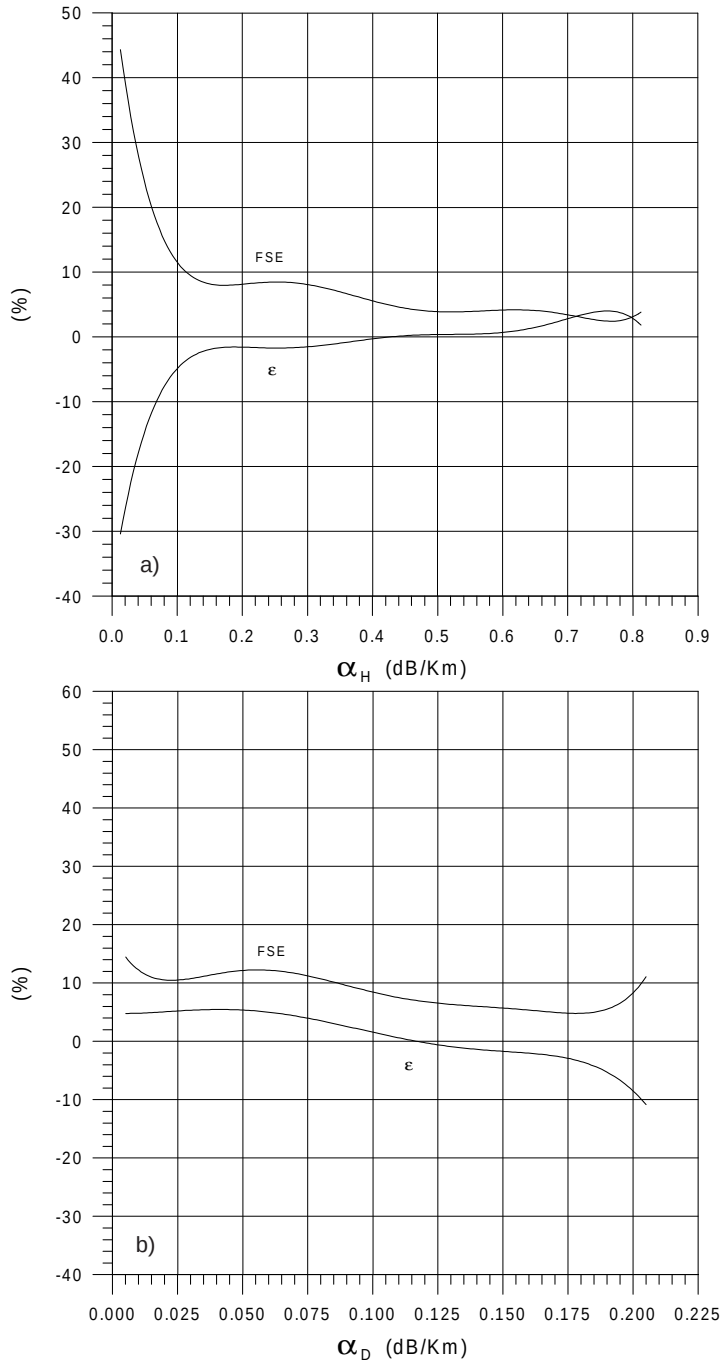

Fig. 3. – *a*) Bias ε and FSE of the $\widehat{\alpha}_{\mathrm{H}}$ estimator, eq. (14*a*), *C*-band, $T = 10\,^{\circ}\mathrm{C}$. *b*) Bias ε and FSE of the $\widehat{\alpha}_{\mathrm{D}}$ estimator, eq. (14*b*), *C*-band, $T = 10\,^{\circ}\mathrm{C}$.

increasing α_H. Instead the values of ε and the FSE for the differential attenuation estimates range between -10 and $+5\%$, and between $+5$ and $+15\%$, respectively.

4. – Rain models and error sources in rainfall rate estimation

The effectiveness of the correction technique for improving rainrate estimates is related to rainfall path between measurement cell and radar. In our analysis we have considered two different rainfall paths:

1) Uniform rainfall rate along the propagation path, where drop size distribution parameters are constant, *i.e.* the DSD parameters (N_0, D_0, μ) are not varied along the path. This model corresponds to a very correlated rain path (type-1 rain).

2) Uniform rainfall rate along the propagation path, where the DSD parameters N_0 and μ are varied randomly following Ulbrich's range (8*a*)-(8*c*) [6], while D_0 is calculated from the inversion of eq. (9):

$$D_0 = (\mu + 3.67)\left[\frac{r^{(\nu)}}{0.6\cdot 10^{-3}\cdot 3.778\cdot N_0\,\Gamma(\mu + 4.67)}\right]^{1/(\mu + 4.67)}. \tag{15}$$

In this second model (type-2 rain) the rain is decorrelated from cell to cell.

The above-described correction attenuation scheme is affected by a set of errors, that we can classify as:

a) *Systematic error sources*, due to bias on Z_H measurements related to the calibration system, or bias on the Z_{DR} measurements due to the mismatching between the radiation diagram at horizontal and vertical polarization. The analysis will be studied in detail in sect. **5**.

b) *Random error sources* related to the physical variability (DSD variation) and statistical variability of the radar observables. In our analysis the statistical signal fluctuations are neglected to evaluate the best-fit relationship errors.

Then the random errors can be decomposed into:

1) best-fit relationship errors due to rainfall rate estimation;

2) best-fit relationship errors due to attenuation estimate;

3) best-fit relationship errors related to attenuation estimate by attenuation-corrected values of Z_H and Z_{DR}.

The errors 1) and 2) have been analyzed in the previous section, while the error 3) and the theoretical and simulated evaluation of the corrected rainfall rate estimation will be the subject of sects. **6** and **7**.

We point out that the correction procedure is not a linear procedure, then the total error is not the sum of errors.

5. – Rainfall rate estimation errors due to biases

Considering biases on absolute and differential reflectivity measurements (B_H and B_{DR}, respectively), with regard to rainrate estimator, eq. (10), the percentage error ε

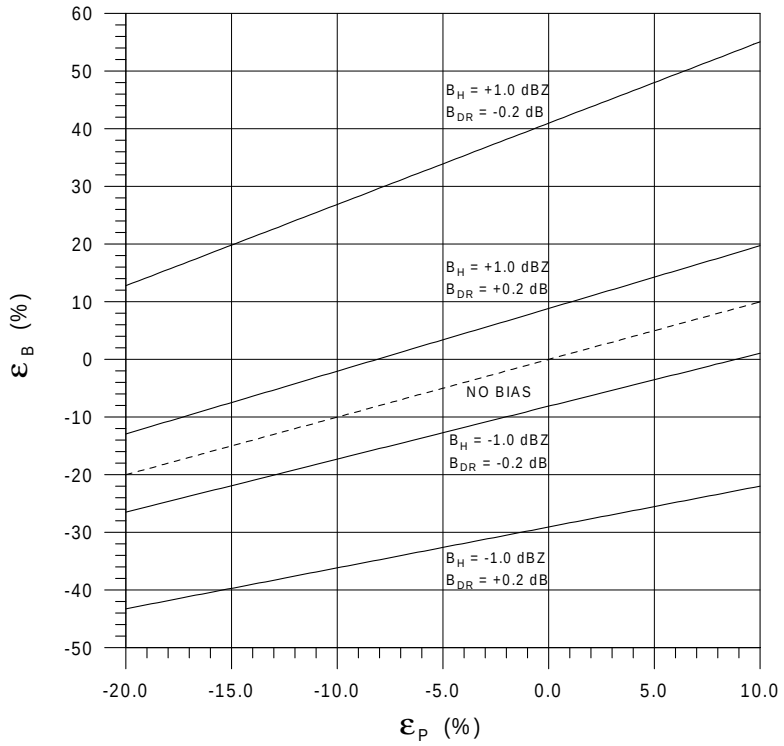

Fig. 4. – Percentage error ε_B due to biases B_H and B_{DR} on Z_H and Z_{DR}, respectively, *vs.* percentage error ε_P due to the best-fit relationship.

can be written as

$$\varepsilon_B = \left[\frac{r^{(b)}}{r^{(v)}} - 1 \right] \cdot 100 = \left[\frac{\beta_r \cdot r^{(p)}}{r^{(v)}} - 1 \right] \cdot 100 \quad (\%), \tag{16}$$

where $r^{(v)}$, $r^{(p)}$ and $r^{(b)}$ are, respectively, the *true* rainrate, the *estimated* rainrate without bias on Z_H and Z_{DR}, the *estimated* rainrate with bias on Z_H and Z_{DR}. The term β_r is equal to $\beta_r = 10^{c_2 B_H - c_3 B_{DR}}$, where B_H and B_{DR} are the biases in dBZ and dB concerning Z_H and Z_{DR}. The percentage error ε_P (no bias) and the percentage error ε_B with bias are connected by the following relationship:

$$\varepsilon_B = \varepsilon_P \beta_r + (\beta_r - 1) \cdot 100 \quad (\%). \tag{17}$$

Figure 4 shows ε_B *vs.* ε_P for some values of B_H and B_{DR}; ε_P is varied between -20 and $+10\%$ according to fig. 2, where the values of ε_P are included between -15 and $+5\%$. Positive bias of the absolute reflectivity and negative bias of the differential reflectivity are the most dangerous leading to high errors in the rainfall rate estimation; this means that the radar should be well calibrated before application of the correction technique.

6. – Theoretical analysis of the rainfall rate estimation error

Considering the *true* absolute and differential attenuation values, eqs. (5) and (6), and the estimate values $\widehat{\alpha}_{\mathrm{H}}$ and $\widehat{\alpha}_{\mathrm{D}}$, eqs. (14*a*), (14*b*), we can write the rainfall rate estimation eq. (10) and the *attenuation-corrected* rainfall rate at the n-th range cell as

$$[r^{(\mathrm{p})}]_n = c_1 \cdot 10^{c_2\left\{[Z_{\mathrm{H}}^{(\mathrm{m})}]_n + 2\sum_{i=1}^{n-1}\alpha_{\mathrm{H}i}\,\Delta x_i\right\} - c_3\left\{[Z_{\mathrm{DR}}^{(\mathrm{m})}]_n + 2\sum_{i=1}^{n-1}\alpha_{\mathrm{D}i}\,\Delta x_i\right\}}, \tag{18}$$

$$[r^{(\mathrm{c})}]_n = c_1 10^{c_2\left\{[Z_{\mathrm{H}}^{(\mathrm{m})}]_n + 2\sum_{i=1}^{n-1}\widehat{\alpha}_{\mathrm{H}i}\,\Delta x_i\right\} - c_3\left\{[Z_{\mathrm{DR}}^{(\mathrm{m})}]_n + 2\sum_{i=1}^{n-1}\widehat{\alpha}_{\mathrm{D}i}\,\Delta x_i\right\}}, \tag{19}$$

where in the first equation the rainrate is estimated using the *true* values of the attenuation, while in the second equation the rainrate is evaluated employing the *estimated* values of the attenuation.

Combining eqs. (18) and (19), at the n-th range cell the percentage error is

$$[\varepsilon]_n = \frac{[r^{(\mathrm{c})}]_n - [r^{(\mathrm{p})}]_n}{[r^{(\mathrm{p})}]_n}\cdot 100 = \left\{10^{c_2\left[2\sum_{i=1}^{n-1}(\widehat{\alpha}_{\mathrm{H}}-\alpha_{\mathrm{H}})_i\Delta x_i\right] - c_3\left[2\sum_{i=1}^{n-1}(\widehat{\alpha}_{\mathrm{D}}-\alpha_{\mathrm{D}})_i\Delta x_i\right]} - 1\right\}\cdot 100\,. \tag{20}$$

If the rain is uniform into the space (type 1), the reflectivity Z_{H} and Z_{DR} and the attenuation α_{H}, $\widehat{\alpha}_{\mathrm{H}}$, and α_{D} $\widehat{\alpha}_{\mathrm{D}}$ are constant along the range, and assuming the cell length equal to Δx, the percentage error can be written as

$$[\varepsilon]_n = \left\{10^{c_2\cdot 2\,\Delta x(n-1)(\widehat{\alpha}_{\mathrm{H}}-\alpha_{\mathrm{H}}) - c_3\cdot 2\,\Delta x(n-1)(\widehat{\alpha}_{\mathrm{D}}-\alpha_{\mathrm{D}})} - 1\right\}\cdot 100 \quad (\%)\,. \tag{21a}$$

$\Delta x(n-1) = L$ is the path propagation length; replacing $x = \widehat{\alpha}_{\mathrm{H}} - \alpha_{\mathrm{H}}$ and $y = \widehat{\alpha}_{\mathrm{D}} - \alpha_{\mathrm{D}}$, we have

$$[\varepsilon]_n = [10^{2L\{c_2 x - c_3 y\}} - 1]\cdot 100 = [\exp[4.605\,L\,(c_2 x - c_3 y)] - 1]\cdot 100\,. \tag{21b}$$

Considering the first-order Taylor approximation around $x = 0$ and $y = 0$, with $c_2 = 0.093$ and $c_3 = 0.281$, eq. (19*b*) becomes

$$[\varepsilon]_n \approx L\,(0.428x - 1.294y)\cdot 100 \quad (\%)\,. \tag{21c}$$

For the type-1 rain the percentage error increases increasing the path length and it depends on two opposite terms.

For the type-2 rain where the DSD parameters are randomly varied with a fixed rainrate, we can write

$$[\varepsilon]_n = \left\{10^{c_2\left[2\sum_{i=1}^{n-1}(\widehat{\alpha}_{\mathrm{H}}-\alpha_{\mathrm{H}})_i\Delta x_i\right] - c_3\left[2\sum_{i=1}^{n-1}(\widehat{\alpha}_{\mathrm{D}}-\alpha_{\mathrm{D}})_i\Delta x_i\right]} - 1\right\}\cdot 100\,, \tag{22a}$$

$$[\varepsilon]_n = \left\{10^{2c_2 L(\bar{\widehat{\alpha}}_{\mathrm{H}} - \bar{\alpha}_{\mathrm{H}}) - 2c_3 L(\bar{\widehat{\alpha}}_{\mathrm{D}} - \bar{\alpha}_{\mathrm{D}})} - 1\right\}\cdot 100\,, \tag{22b}$$

$$[\varepsilon]_n \approx L\,(0.428\bar{x} - 1.294\bar{y})\cdot 100\,. \tag{22c}$$

Equation (22*c*) is similar to eq. (21*c*), the quantities $\bar{x}$ and $\bar{y}$ represent the difference of the mean values (*true* and *estimated*) of the specific absolute and differential attenuation along the propagation path.

In fig. 5 the plots of eqs. (21*c*) and (22*c*) *vs. estimated* rainrate are plotted (continuous line: type-1 rain; dotted line: type-2 rain). An underestimate of the

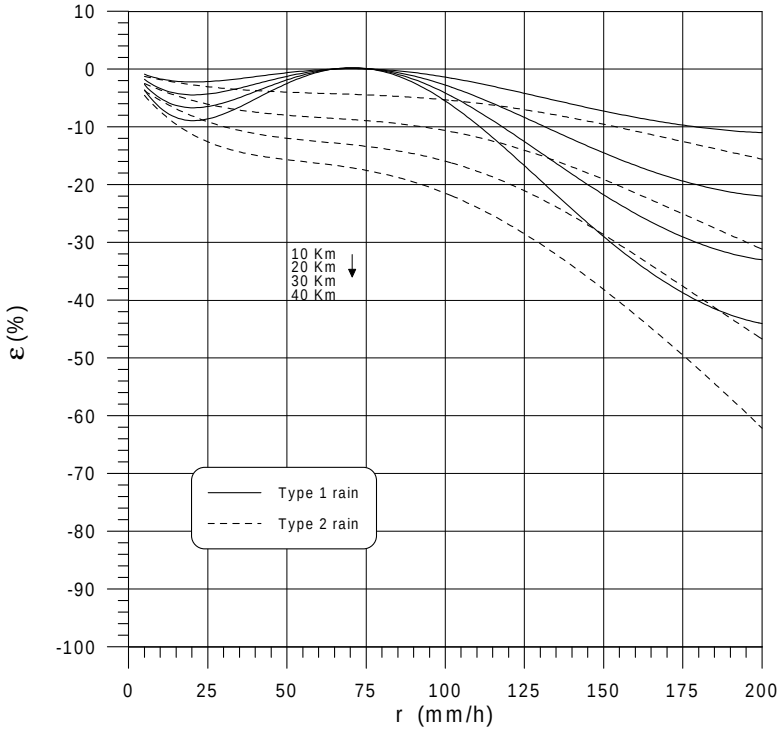

Fig. 5. – Theoretical approximation of the percentage error ε, eqs. (21*c*) and (22*c*), of the attenuation-corrected rainrate estimation. Solid line: type-1 rain; dotted line: type-2 rain.

attenuation-corrected rainrate is inferred; it increases with increasing rainfall rate and path length.

We point out that in every range cell the estimates of the attenuation are computed using the *true* values of the absolute and differential reflectivity. In practice at the i-th range cell, absolute and differential attenuation are estimated by corrected values of Z_{H} and Z_{DR} values corresponding to the previous cells. In this way, a further error is introduced in the rainfall rate estimation, and will be discussed in the following sect. **7**.

7. – Evaluation of the results

A wide set of results by computer simulation are shown in the following. In the simulation the drop size distribution parameters are varied as described in sect. **2**. The values of the path length have been considered equal to 10, 20, 30 and 40 km; while the number of range cells N_{C} has been supposed equal to 10.

For the type-1 and type-2 rain models the percentage error (ε) and the Fractional Standard Error (FSE) *vs.* the rainrate obtained by the best-fit relationship, eq. (10), have been evaluated for:

a) *measured rainfall rate* (equal to attenuated value);

b) *attenuation-corrected rainfall rate estimation*, where the absolute and differential attenuation estimates have been derived using the *corrected* values of Z_H and Z_{DR}.

Subsequently, the results concerning points *a*) and *b*) have been compared with the results derived using a K_{DP} estimator. In this last case the rainrate is estimated by the differential phase shift which is a non-attenuated observable.

7˙1. *Errors in the measured rainfall rate.* – In figs. 6*a* and 6*b* the percentage error ε and the FSE of the *measured* (attenuated) rainrate *vs.* the best-fit estimated rainrate (non-attenuated) are plotted (continuous line: type-1 rain; dotted line: type-2 rain). The length of the propagation path is a parameter.

The following conclusion can be drawn. The percentage error and the FSE have a very increasing trend when the rainrate and the propagation path increase. For example, with a path equal to 10 km (type-1 rain) the percentage error is up to 50% when the rainrate is greater than 150 mm/h. This value is reduced to 85 mm/h for a path equal to 20 km, to 60 mm/h for a path of 30 km and is equal to 40 mm/h for a distance of 40 km.

For the type-2 rain model the percentage error and the FSE are greater in comparison with type-1 rain.

From figs. 6*a* and 6*b* we conclude that the attenuation has to be corrected in order to reduce the estimate rainrate error even if the propagation path length is short (10 km).

7˙2. *Errors in the corrected rainrate using corrected values of Z_H and Z_{DR}.* – In this section we analyzed the attenuation compensation technique when the estimate of α_H and α_D are computed using the *attenuation-corrected* values of reflectivity Z_H and Z_{DR}.

The convergence of the proposed compensation attenuation algorithm (see sect. **3**) depends on the estimates of $\widehat{\alpha}_H$ and $\widehat{\alpha}_D$. In fact if the absolute attenuation is overestimated and the differential attenuation is underestimated, the *attenuation-corrected* rainrate diverges assuming very high values; on the contrary, if the differential attenuation is overestimated and the absolute attenuation is underestimated, the *attenuation-corrected* rainrate converges to *zero*. The combination of over- and underestimation of α_H and α_D produces the trend of the errors in the corrected rainfall rate estimation. Remember that the best-fit relationship (Z_H, Z_{DR}) used to estimate the attenuation α_H and α_D has been computed with a fixed range for Z_H and Z_{DR}. If sometimes the corrected values of Z_H and Z_{DR} are out of the valid range, the estimates of α_H and α_D can be completely wrong and can cause an erroneous estimate of r.

Figures 7*a*, 7*b* show the results for the two types of rain. For example, with a path of 10 km the FSE is limited inside 30% for all precipitation values.

For the type-2 rain (DSD is changed from cell to cell) an average effect is generated in the estimated attenuation so that the errors, *vs.* rainrate, are generally more regular.

7˙3. *Comparison between different radar rainfall rate algorithms.* – In this subsection a comparison among the FSE of estimates with and without the attenuation-

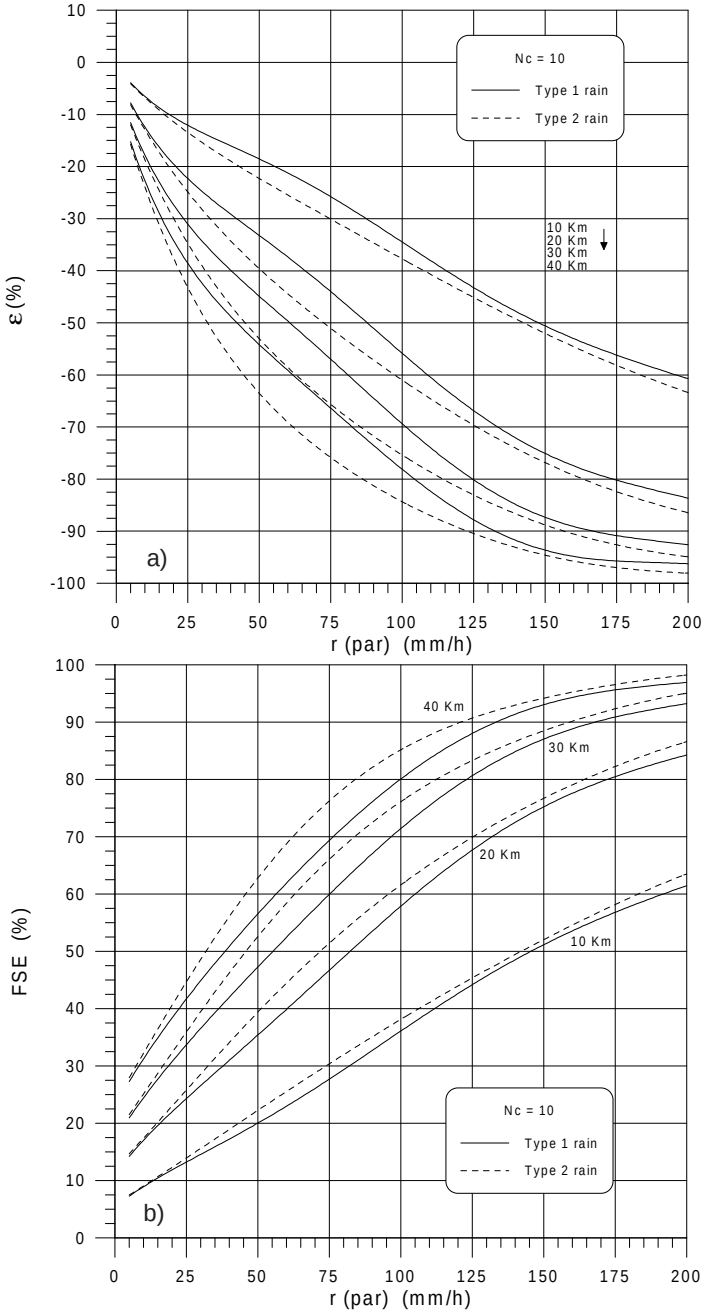

Fig. 6. – *a*) Percentage error ε of the rainrate estimation when Z_H and Z_{DR} are attenuated *vs.* the parametrized rainrate estimation r(par). Solid line: type-1 rain; dotted line: type-2 rain. Path 10, 20, 30 and 40 km. *b*) FSE of the rainrate estimation when Z_H and Z_{DR} are attenuated *vs.* the parametrized rainrate estimation r(par). Symbols as in *a*).

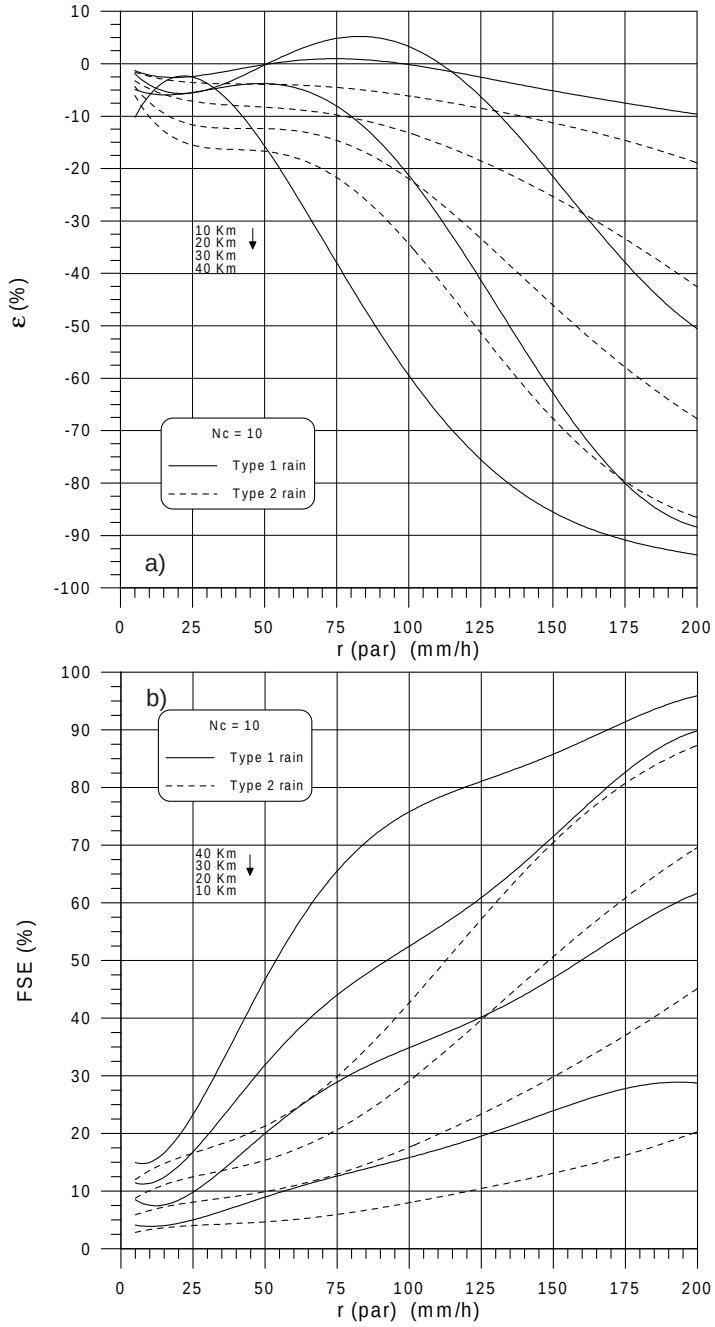

Fig. 7. – *a*) Percentage error ε of the attenuation-corrected rainrate estimation *vs.* the parametrized rainrate estimation r(par). Solid line: type-1 rain; dotted line: type-2 rain. Path 10, 20, 30 and 40 km. *b*) FSE of the attenuation-corrected rainrate estimation *vs.* the parametrized rainrate estimation r(par). Symbols as in *a*).

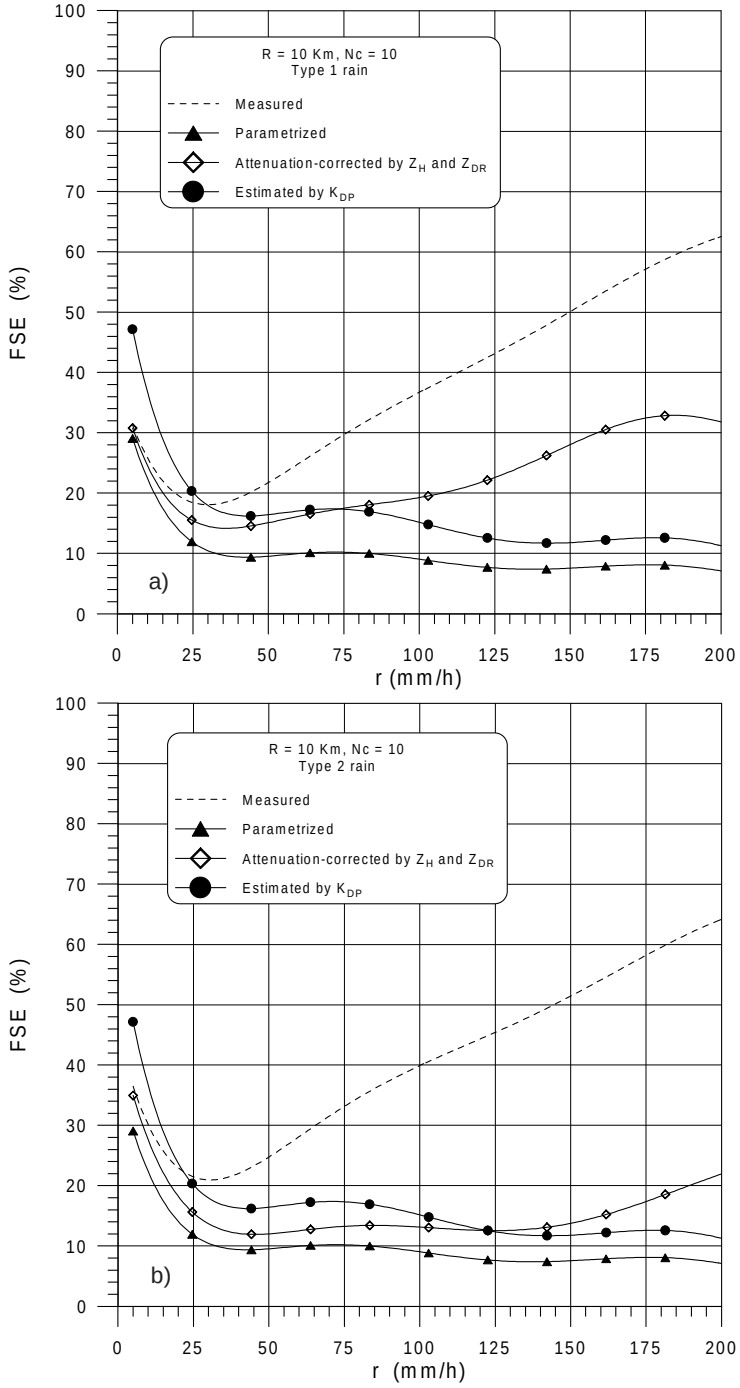

Fig. 8. – *a*) FSE comparison between different radar rainfall rate estimates. Type-1 rain. Path 10 km. $N_C = 10$. *b*) Type-2 rain.

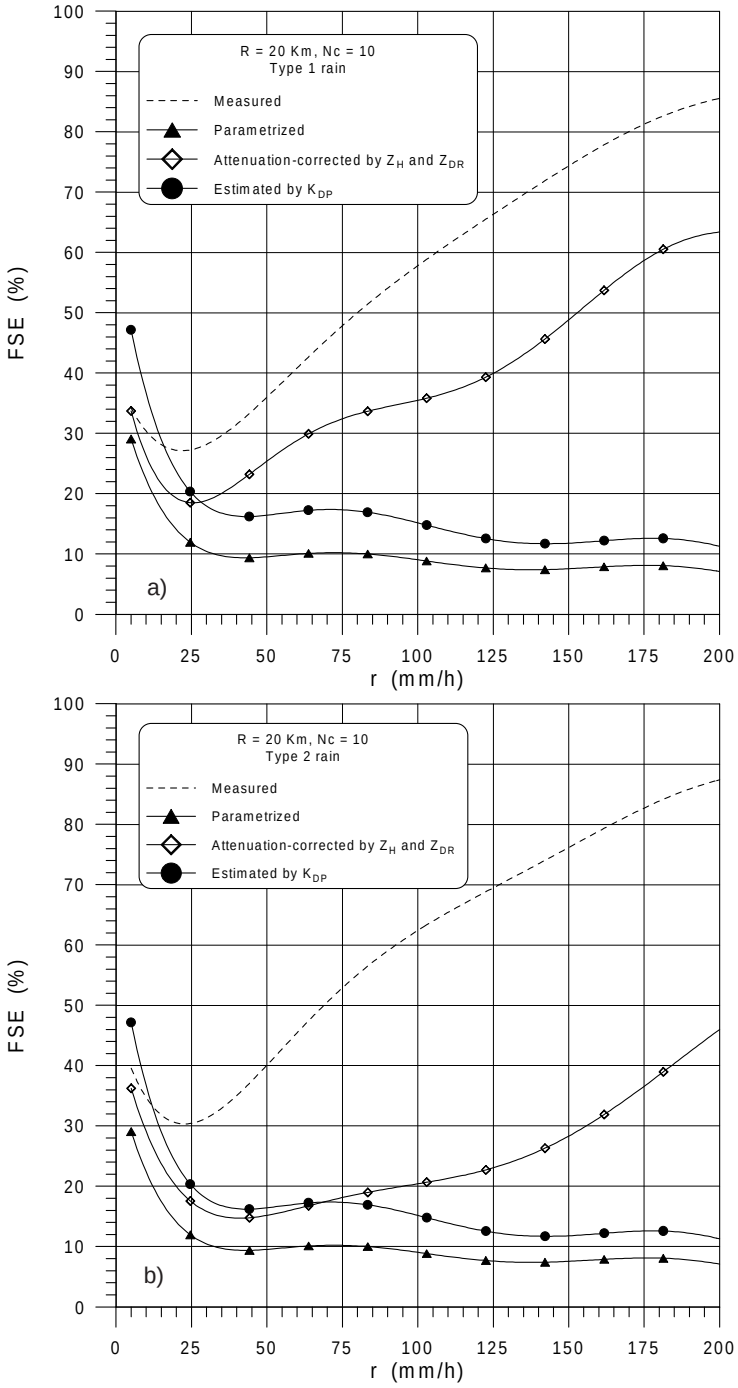

Fig. 9. – *a*) FSE comparison between different radar rainfall rate estimates. Type-1 rain. Path 20 km. $N_C = 10$. *b*) Type-2 rain.

correction and the estimate rainrate by K_{DP} is proposed to characterize the range of precipitaion in which it is useful to employ the attenuation compensation technique or estimate directly r by K_{DP} measurements. The *parametrized* rainfall rate eq. (10) is added. The evaluations are referred to the *true* rainfall rate.

For the type-1 rain with a propagation path of 10 km, in fig. 8*a* the FSE *vs.* the *true* rainrate are plotted. If the *measured* rainrate is lower than 15 mm/h it is not useful to employ the attenuation compensation algorithm. When r is greater than 15 mm/h and smaller than 75 mm/h, it is suitable to correct the attenuation by Z_H and Z_{DR} observables. The differential phase shift K_{DP} is used to estimate r when the rainrate is greater than 75 mm/h.

In the same conditions for the type-2 rain, fig. 8*b* suggests that: for rainrate lower than 10 mm/h it is not necessary to compensate the attenuation. For rainrate greater than 10 mm/h and lower than 120 mm/h it is useful to employ Z_H and Z_{DR} for correcting the attenuation phenomena; when r is greater than 120 mm/h the K_{DP} method is favourite in the rainfall rate estimation.

If the propagation path is doubled (20 km) with the same sampling in range, the results, for the two types of rain, are shown in figs. 9*a* and 9*b*, respectively. The graphs are similar to the previous case. In particularly, for the type-1 rain if the measured precipitation r is smaller than 5 mm/h the attenuation compensation is not needed. For rainrate grater than 5 mm/h and lower than 30 mm/h it is useful to correct the attenuation by Z_H and Z_{DR} observables. When the rainrate is greater than 30 mm/h it is suitable to estimate r using K_{DP} measurement.

For type-2 rain and for rainrate lower than 5 mm/h the compensation attenuation is not necessary; when r is greater than 5 mm/h and smaller than 70 mm/h it is useful to employ Z_H and Z_{DR} to correct the attenuation. For rainrate greater than 70 mm/h a direct estimation of rainfall rate by K_{DP} measurement is advisable.

All results have been derived with a number of range cells N_C equal to 10. On changing N_C along the propagation path considerable variations have not been noticed.

8. – Conclusions

The effectiveness of an attenuation correction procedure on the error structure of a *C*-band radar rainfall estimation is studied theoretically and by computer simulation.

The iterative procedure to correct the radar observables Z_H and Z_{DR} for the absolute and differential attenuation is based on the best-fit relationships between the (Z_H, Z_{DR}) and the specific absolute and differential attenuation α_H, α_D).

In the first part we have theoretically examined the accuracy of the technique for two different types of rain medium. In the first type, the rain path is uniform and the drop size distribution parameters (N_0, D_0, μ) remain constant from cell to cell, while in the second type, N_0, D_0, μ are varied from cell to cell (a physically more realistic situation). The *random* errors due to the variability of the DSD and the *systematic* errors have been analyzed. In our analysis the effects of measurements error due to signal fluctuations have been neglected; in any case these errors can be minimised using opportune time-space averages.

The results have shown that the application of the attenuation compensation technique produces a negative bias in the rainfall rate estimation. The bias increases

increasing the propagation path and the rainfall rate, while it is little sensitive to the number of cells along the propagation path with a fixed range.

In the last part of this work the range of precipitation values have been derived in which it is useful to compensate the attenuation or directly to estimate the rainrate by K_{DP} measurement.

In the more realistic case (type-2 rain with a path length equal to 10 km) we have shown that for the *measured* rainrate lower than 10 mm/h the attenuation compensation is not necessary. For $10 < r < 120$ mm/h it is useful to apply the correction technique. When the rainrate is greater than 120 mm/h, the K_{DP}-based technique is favourite in the rainfall rate estimation.

Increasing the propagation path, the application of the compensation technique involves an underestimation of the rainfall rate; in this case the use of K_{DP} relationship is suitable.

With regard to it we point out that the direct estimate of r using K_{DP} is independent of the calibration and the attenuation phenomena; yet in our analysis the back-scattering contribution (δ) in the differential phase shift estimate has been neglected; however this effect can be reduced by a suitable filtering.

In conclusion, the attenuation technique, generally, has shown a good behaviour. Operational limits of this technique are, of course, related to the length of rain-filled paths and very high values of rainfall because, in this case, the best-fit relationships are affected by high errors. However, before applying the correction procedure we have shown that the radar should be well calibrated for Z_H and Z_{DR} measurements.

Finally, we have shown that the direct use of K_{DP} (non-attenuated observable) to estimate the rainrate is useful particularly when the rainfall rate is very high.

REFERENCES

[1] DOVIAK R. J. and ZRNIC D. S., *Doppler Radar and Weather Observation* (Academic Press, Inc.) 1984, pp. 39-42.

[2] HILDEBRAND P. H., *Iterative correction for attenuation of 5 cm radar in rain, J. Appl. Meteorol.*, **17** (1978) 508-514.

[3] AYDIN K., SELIGA T. A. and ZHAO Y., *A self-correction procedure of attenuation due to rain for C band dual linear polarization radars, 23rd Conference on Radar Meteorology* (*Snowmass, CO*), in *Am. Meteorol. Soc.*, **3** (1986) JP337-JP341.

[4] AYDIN K., SELIGA T. A. and ZHAO Y., *Rain induced attenuation effects on C band dual polarization meteorological radars, IEEE Transact. Geosci. Remote Sensing*, **27** (1989) 57-65.

[5] GORGUCCI E., SCARCHILLI G. and CHANDRASEKAR V., *Radar and raingage measurements of rainfall over the Arno basin, Conference on Hydrology, 15-20 January 1995, Dallas, Texas, Am. Meteorol. Soc.*, 1993, pp. 68-73.

[6] ULBRICH C. W., *Natural variations in the analytical form of raindrop size distribution, J. Clim. Appl. Meteor.*, **22** (1983) 1774-1775.

[7] SCARCHILLI G., GORGUCCI E., CHANDRASEKAR V. and SELIGA T. A., *Rainfall estimation using polarimetric techniques at C band frequencies, J. Appl. Meteorol.*, **32** (1993) 1150-1160.